

MultiNash-PF: A Particle Filtering Approach for Computing Multiple Local Generalized Nash Equilibria in Trajectory Games

Maulik Bhatt¹ Iman Askari² Yue Yu³ Ufuk Topcu⁴ Huazhen Fang² Negar Mehr¹

Abstract—Modern-world robotics involves complex environments where multiple autonomous agents must interact with each other and other humans. This necessitates advanced interactive multi-agent motion planning techniques. Generalized Nash equilibrium(GNE), a solution concept in constrained game theory, provides a mathematical model to predict the outcome of interactive motion planning, where each agent needs to account for other agents in the environment. However, in practice, multiple local GNEs may exist. Finding a single GNE itself is complex as it requires solving coupled constrained optimal control problems. Furthermore, finding all such local GNEs requires exploring the solution space of GNEs, which is a challenging task. This work proposes the MultiNash-PF framework to efficiently compute multiple local GNEs in constrained trajectory games. Potential games are a class of games for which a local GNE of a trajectory game can be found by solving a single constrained optimal control problem. We propose MultiNash-PF that integrates the potential game approach with implicit particle filtering, a sample-efficient method for non-convex trajectory optimization. We first formulate the underlying game as a constrained potential game and then utilize the implicit particle filtering to identify the coarse estimates of multiple local minimizers of the game's potential function. MultiNash-PF then refines these estimates with optimization solvers, obtaining different local GNEs. We show through numerical simulations that MultiNash-PF reduces computation time by up to 50% compared to a baseline approach.

I. INTRODUCTION

Modern-world robotics applications are inherently multi-agent in nature. For instance, autonomous cars on highways need to account for other vehicles while planning their motion. Many robotics applications require motion planning for selfish agents sharing a common operational space, such as autonomous cars and delivery robots. In such settings, autonomous agents should account for other agents in the shared environment while achieving their individual goals. Autonomous agents need to reason about the impact of their actions on other agents. Game theory provides a formal way to deal with such interactive scenarios [1]. Furthermore, recent works have shown that game-theoretic trajectory planning makes robots more socially acceptable to humans [2].

To model the outcome of such interactive scenarios, Nash equilibrium is a key concept in game theory. When multiple

¹Maulik Bhatt and Negar Mehr are with Department of Mechanical Engineering, University of California, Berkeley, CA, 94720, USA {maulikbhatt,negar}@berkeley.edu

²Iman Askari and Huazhen Fang are with University of Kansas, Lawrence, KS, 66045, USA {askari,fang}@ku.edu

³ Yue Yu is with University of Minnesota, Minneapolis, 55455, USA yuey@umn.edu

⁴ Ufuk Topcu is with University of Texas at Austin, TX, 78712, USA utopcu@utexas.edu

agents- such as robots and humans- interact, a Nash equilibrium corresponds to a joint action such that no agent has incentives to deviate from its equilibrium actions unilaterally. This allows us to account for agents' individual preferences when interacting in a common environment. We formulate a multi-agent interactive trajectory planning problem as a *trajectory game*. In robotics, seeking Nash equilibria of the underlying trajectory games has been proven to be effective [3], [4]. Furthermore, in real-world applications, agents may have to satisfy some safety constraints, such as avoiding collisions with obstacles and other agents in the environment. In such constrained multi-agent interactive settings, the interaction outcomes are captured through *generalized Nash equilibrium*(GNE), which are constrained Nash equilibria. Several recent works have shown great success in utilizing GNE for multi-agent motion planning in interactive domains [5], [6].

However, in practice, multiple local GNEs may exist for a trajectory game. For example, in the two-player trajectory game illustrated in Fig. 1, the agents need to move towards their goals while avoiding collisions. Here, two local GNEs exist: clockwise trajectories and counterclockwise trajectories. If the two agents were to act independently, they could reach different GNEs, which would result in a collision. Therefore, agents need a coordination mechanism to avoid such scenarios. However, identifying all the possible local GNEs is required to enable effective coordination. Therefore, computing multiple local GNEs is critical to aligning players' preferences over different equilibria [7] or helping coordinate players' actions via recommendation [8]. Furthermore, different local GNEs correspond to different modes of interactions in multi-agent interactive settings. Therefore, it is essential to efficiently recover all the possible *multi-modal* outcomes of multi-agent interactions.

Computing different local GNEs requires an efficient way to solve games. In practice, computing even a single GNE is often challenging [9] because solving for GNE amounts to solving a set of coupled constrained optimal control problems. Typically, such a solution requires solving first-order KKT conditions of the underlying problems. Therefore, solving the GNE often reduces to addressing a set of complementarity conditions, a process known to be computationally demanding, especially for large-scale applications [10]. Furthermore, computing all the different local GNEs requires initializing the game solvers with many different initial guesses of the equilibrium trajectories from prior knowledge of the specific scenario. Further, as the number of participating agents increases, the dimension of

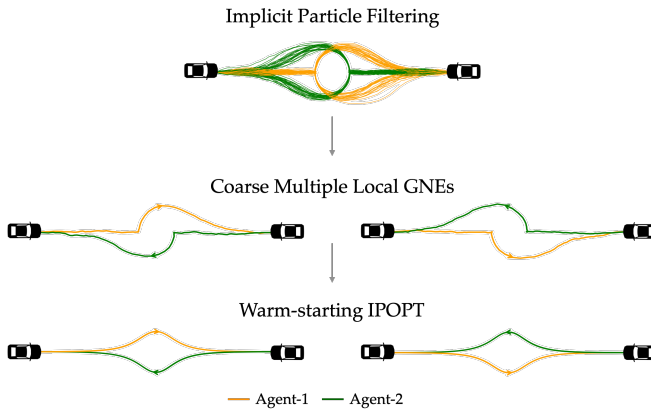


Fig. 1: The Nash equilibrium trajectories found by *MultiNash-PF* when two unicycle agents change their positions. First, we use the implicit particle filter to discover the coarse estimates of two different equilibria, and then utilize them as a warm starting for IPOPT to obtain the two Nash equilibrium trajectories.

the nonconvex optimization grows to interactable levels. This further increases the required number of initial guesses for the game solvers to find all local GNEs. To our best knowledge, there is no principled approach to compute multiple local Nash equilibria in constrained trajectory games other than exhaustive random initializations of the game solvers.

We propose a novel framework named *MultiNash-PF* to efficiently compute multiple local GNEs in constrained trajectory games. The approach combines

- 1) constrained potential games [11], a class of games for which we can compute local Nash equilibria by optimizing a single constrained optimal control problem, and,
- 2) constraint aware implicit particle filtering, which is a sample-efficient particle filtering method recently used for nonconvex trajectory optimization [12].

Using constrained potential games, it is possible to compute a local GNE by solving a constrained optimal control problem using off-the-shelf optimization solvers. These solvers outperform state-of-the-art constrained dynamic game solvers in computation speed during [13]. After formulating the constrained trajectory game as a constrained potential game, our approach employs the constraint-aware implicit particle filtering method to identify multiple local minima of the potential game. This method eliminates the requirements of random initialization of the optimization solver by efficiently obtaining coarse estimates of different local GNEs. Next, we use the identified minima as initialization for the optimization solver. The solver then computes all the different local GNEs of the original game. The framework of *MultiNash-PF* is depicted in Fig. 1. Leveraging the sample efficiency of the implicit particle filtering method, *MultiNash-PF* can explore and identify the multiple local GNEs faster than the random initialization of optimization solvers.

II. RELATED WORKS

Game Theoretic Planning. One of the earliest works laying the foundation of game theoretic motion planning was

[14]. Game theoretic motion planners that seek Stackelberg equilibria were proposed in [15], [3]. Later, methods that seek Nash equilibria were developed. These methods differ mainly in the way they compute Nash equilibria. Iterative best response methods for computing Nash equilibria were developed in [16], [17]. Iterative linear quadratic approximations to compute Nash equilibria were introduced in [18]. ALGames was developed in [19] which is an augmented lagrangian-based solver for constrained dynamic games. A sequential linear-quadratic technique game-based technique to compute GNE was proposed in [20]. However, these methods are computationally expensive for real-time implementations as the number of agents increases. Potential games-based methods were developed later in [11], [21], [13], [22] to reduce the complexity of computing equilibria. However, the shortcomings of all these methods lie in the fact that they find only one Nash equilibrium of the underlying game and ignore the multi-modal nature of the problem that is crucial for coordination among agents. In [7], the authors recognize the existence of multiple equilibria and focus on inferring the equilibrium of other agents in the environment. However, the methodology relies on computing the different approximate local Nash by rollouts of randomly selected initial strategies, which we show in this work to be computationally intractable with the risk of not identifying all possible equilibria.

Multiple Local Solutions to Constrained Optimal Control. In general, optimal control problems are often formulated as nonconvex constrained optimization problems, which are solved through the conventional gradient-based approaches such as inter-point methods [23] and sequential quadratic programming [24]. However, given an initialization, they can only find a single local optimal solution. However, in the present context of identifying all potential local GNEs, the gradient-based method would require numerous initializations to find all the local solutions. Departing from gradient-based methods, a Bayesian inference approach has been proposed to solve model predictive control problem [25], [26], [27]. The approach formulates the optimal control problem from a Bayesian inference perspective and employs particle filtering as its estimation method. At its core, particle filtering utilizes sequential Monte Carlo sampling to perform state estimation for highly nonlinear systems [28], [29]. The efficiency and accuracy of the estimation largely depend on the quality of the sampled particles. Recently, in [30], an efficient particle filtering method was proposed based on the principle of implicit sampling. This sampling approach relies on the premise that a few particles are required for accurate estimation if the particles are sampled from high-probability regions of the probability distribution function. In addition, the implicit sampling technique can also mitigate the need for a resampling step to avoid filter collapse.

III. MULTI-AGENT CONSTRAINED TRAJECTORY GAMES

We formulate the multi-agent interactive trajectory planning problem as an N -agent constrained trajectory game. Let

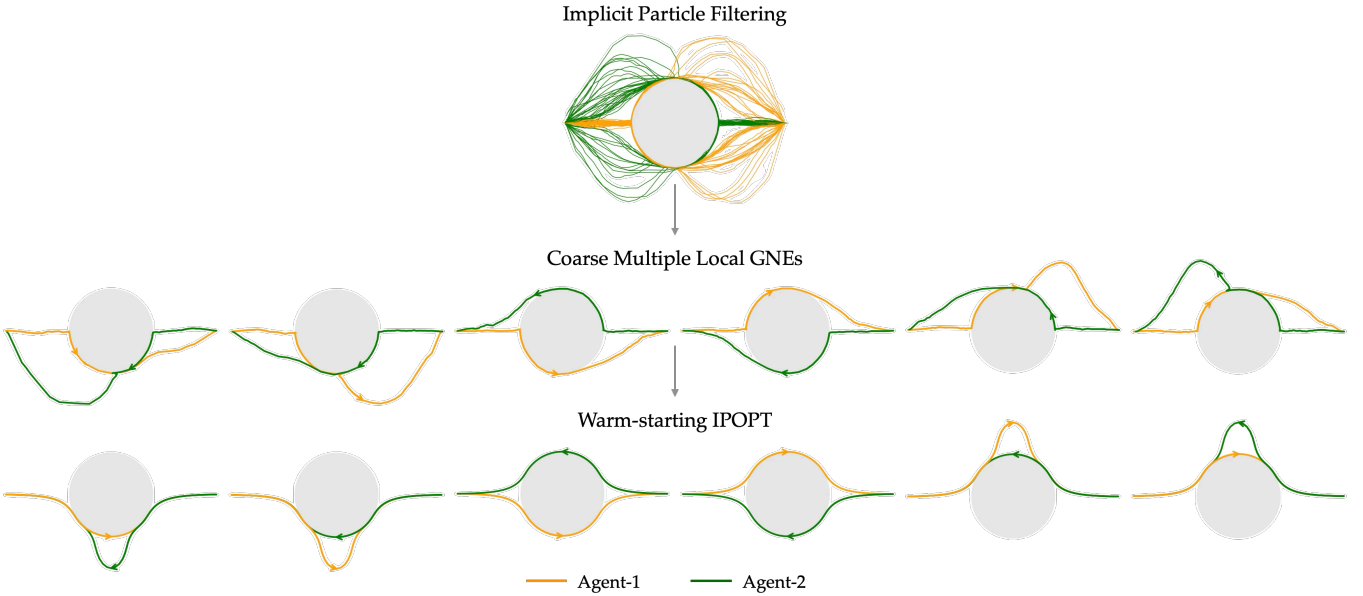


Fig. 2: MultiNash-PF identifies all the local GNE trajectories for a challenging two agent trajectory game where two agents swapped positions while avoiding an obstacle. In this scenario, the obstacle radius is greater than the collision avoidance radius of the two agents, leading to the discovery of 6 distinct Nash equilibria. MultiNash-PF effectively obtains coarse estimates of local GNEs through implicit particle filtering, which are then refined using IPOPT to obtain local GNEs.

$\mathcal{N} := \{1, 2, \dots, N\}$ denote the set of agents' indices. We assume that the game is played over a finite time horizon of $\tau \in \mathbb{N}$ time-steps, where \mathbb{N} is the set of natural numbers.

Let $x_t^i \in \mathbb{R}^{n_i}$ and $u_t^i \in \mathbb{R}^{m_i}$ denote the state and control of the i -th agent at time t , respectively. We assume that the state of the i -th agent evolves as follows:

$$x_{t+1}^i = f^i(x_t^i, u_t^i), \quad (1)$$

for all $t \leq \tau$, where $f^i : \mathbb{R}^{n_i} \times \mathbb{R}^{m_i} \rightarrow \mathbb{R}^{n_i}$ is a continuously differentiable function characterizing the dynamics of the i -th agent. Let $n = \sum_{i=1}^N n_i, m = \sum_{i=1}^N m_i$. We denote the joint state, input, and dynamics of all agents as $x_t := [(x_t^1)^\top \ (x_t^2)^\top \ \dots \ (x_t^N)^\top]^\top$, $u_t := [(u_t^1)^\top \ (u_t^2)^\top \ \dots \ (u_t^N)^\top]^\top$, and $f := [(f^1)^\top \ (f^2)^\top \ \dots \ (f^N)^\top]^\top$ respectively. Note that each f^i is a vector-valued dynamics function for each agent. Therefore, $f : \mathbb{R}^n \times \mathbb{R}^m \rightarrow \mathbb{R}^n$ will be a vector-valued dynamics function for the joint system.

In constrained trajectory games, each agent has to satisfy some constraints that couple different agents' states and controls and, in general, depend on other agents' states and actions. Let $g : \mathbb{R}^n \times \mathbb{R}^m \rightarrow \mathbb{R}^c$ with $c \in \mathbb{N}$ denote a continuously differentiable function that defines the constraints on the joint state x_t and joint control u_t at each time:

$$g(x_t, u_t) \leq 0_c, \quad (2)$$

where 0_c is a vector of zeros in \mathbb{R}^c . The aim of the constraint function g is to capture individual agents' strict preferences, such as constraints for each agent avoiding obstacles, or avoiding collision with other agents.

We assume that each agent i aims to minimize an objective function. Let Q^i and Q_τ^i be positive semidefinite and R^i be positive definite matrices for all $i \in \mathcal{N}$. We assume that each

agent i seeks to minimize the following objective:

$$\frac{1}{2} \|x_\tau^i - \hat{x}_\tau^i\|_{Q_\tau^i}^2 + \frac{1}{2} \sum_{t=0}^{\tau-1} \|x_t^i - \hat{x}_t^i\|_{Q^i}^2 + \frac{1}{2} \sum_{t=0}^{\tau} \|u_t^i\|_{R^i}^2 \quad (3)$$

where $\hat{x}_t^i \in \mathbb{R}^{n_i}$ is the reference state for agent i at time t . Typically, the reference states for each agent is a path of minimum cost they would follow in the absence of other agents in the environment, e.g., a straight line connecting the start and goal location. Furthermore, we denote the joint reference state of all agents at time t as \hat{x}_t . We use $\text{blkdiag}(A_1, \dots, A_n)$ to denote the block-diagonal of the matrices A_1, \dots, A_n . Let $a_{0:\tau} := \{a_0, \dots, a_\tau\}$ denote the collection of vectors a_t 's over the entire horizon $0 \leq t \leq \tau$. We use $\{x_{0:\tau}^i, u_{0:\tau}^i\}_{i=1}^N$ to denote joint trajectories of all N agents across all times. Note that using the joint notation, we can equivalently write the joint trajectories of all agents as $\{x_{0:\tau}, u_{0:\tau}\}$.

A. Local Generalized Nash Equilibrium Trajectories

Due to the interactive nature of the problem, generally, it is not possible for all agents to minimize their costs simultaneously while satisfying the constraints. Therefore, the interaction outcome is best captured by *local GNE trajectories* of the underlying trajectory game. With dynamics as (1) and constraints as (2), we denote the game in the compact form by

$$\mathcal{G} := (\mathcal{N}, \{Q^i\}_{i \in \mathcal{N}}, \{Q_\tau^i\}_{i \in \mathcal{N}}, \{R^i\}_{i \in \mathcal{N}}, g, f, \hat{x}_{0:\tau}).$$

For a given ϵ , we define the set of local trajectories around a joint trajectory as $\mathcal{D}(\{x_{0:\tau}, u_{0:\tau}\}, \epsilon) = \left\{ \{x'_{0:\tau}, u'_{0:\tau}\} \mid \sum_{t=0}^{\tau} (\|x_t - x'_t\|_2^2 + \|u_t - u'_t\|_2^2) \leq \epsilon \right\}$. A local GNE trajectory for the game \mathcal{G} is then defined as follows.

Definition 1. A set of joint trajectories $\{x_{0:\tau}^{i*}, u_{0:\tau}^{i*}\}_{i=1}^N$ is a local GNE trajectory for \mathcal{G} if for all agent $i \in \mathcal{N}$, agent i 's trajectory $\{x_{0:\tau}^{i*}, u_{0:\tau}^{i*}\}$ is an optimal solution of the following optimization problem within a local neighborhood $\mathcal{D}(\{x_{0:\tau}^*, u_{0:\tau}^*\}, \epsilon)$ for some $\epsilon > 0$:

$$\begin{aligned} \underset{\{x_{0:\tau}^i, u_{0:\tau}^i\}}{\text{minimize}} \quad & \frac{1}{2} \|x_\tau^i - \hat{x}_\tau^i\|_{Q_\tau^i}^2 + \frac{1}{2} \sum_{t=0}^{\tau-1} \|x_t^i - \hat{x}_t^i\|_{Q^i}^2 \\ & + \frac{1}{2} \sum_{t=0}^{\tau} \|u_t^i\|_{R^i}^2 \\ \text{subject to} \quad & x_0^i = \hat{x}_0^i, \quad x_{t+1}^i = f^i(x_t^i, u_t^i), \quad 0 \leq t \leq \tau-1, \\ & g(\tilde{x}_t, \tilde{u}_t) \leq 0_c, \quad 0 \leq t \leq \tau, \end{aligned} \quad (4)$$

where we use the following notation in $g(\tilde{x}_t, \tilde{u}_t)$

$$\begin{aligned} \tilde{x}_t &:= [(x_t^{1*})^\top \ (x_t^{2*})^\top \ \dots \ (x_t^{i-1*})^\top \ (x_t^i)^\top \ (x_t^{i+1*})^\top \ \dots \ (x_t^{N*})^\top]^\top, \\ \tilde{u}_t &:= [(u_t^{1*})^\top \ (u_t^{2*})^\top \ \dots \ (u_t^{i-1*})^\top \ (u_t^i)^\top \ (u_t^{i+1*})^\top \ \dots \ (u_t^{N*})^\top]^\top. \end{aligned}$$

Intuitively, at a local GNE, no agent can reduce their cost function by independently changing their trajectory to any alternative feasible trajectory within a local neighborhood of the joint equilibrium trajectory, $\{x_{0:\tau}^{i*}, u_{0:\tau}^{i*}\}_{i=1}^N$. Note that in generalized Nash equilibria, the agents' trajectories are coupled both through their independent objective functions and their joint constraints. It is important to highlight that solving (4) requires solving a set of N coupled constrained optimal control problems, which is often computationally expensive. Therefore, finding all the local Nash equilibria of the game can be time-consuming when using traditional game theoretic methods that aim to solve coupled optimal control problems. Hence, in order to alleviate this problem, we leverage constrained potential games, which we build on to identify different modes of interaction.

IV. CONSTRAINED TRAJECTORY POTENTIAL GAMES

Constrained trajectory potential games are a class of games for which a GNE of the original game can be computed by optimizing a single constrained optimal control problem called *Potential*, as described in [13]. This reduces the computational cost of computing the GNEs of the game. In the following, we will prove that game \mathcal{G} can be expressed as a constrained trajectory potential game. The following theorem shows that any local minimizer of such a potential function is a local generalized Nash equilibrium trajectory.

Theorem 1. A set of joint trajectories $\{x_{0:\tau}^{i*}, u_{0:\tau}^{i*}\}_{i=1}^N$ is a local GNE trajectory if within a local neighborhood $\mathcal{D}(\{x_{0:\tau}^*, u_{0:\tau}^*\}, \epsilon)$, it is an optimal solution of

$$\begin{aligned} \underset{\{x_{0:\tau}, u_{0:\tau}\}}{\text{minimize}} \quad & \frac{1}{2} \|x_\tau - \hat{x}_\tau\|_{Q_\tau}^2 + \frac{1}{2} \sum_{t=0}^{\tau-1} \|x_t - \hat{x}_t\|_Q^2 \\ & + \frac{1}{2} \sum_{t=0}^{\tau} \|u_t\|_R^2 \\ \text{subject to} \quad & x_0 = \hat{x}_0, \quad x_{t+1} = f(x_t, u_t), \quad 0 \leq t \leq \tau-1, \\ & g(x_t, u_t) \leq 0_c, \quad 0 \leq t \leq \tau, \end{aligned} \quad (5)$$

for some $\epsilon > 0$, where $Q_\tau := \text{blkdiag}(Q_\tau^1, \dots, Q_\tau^N)$, $Q := \text{blkdiag}(Q^1, \dots, Q^N)$ and $R := \text{blkdiag}(R^1, \dots, R^N)$.

Proof. This theorem follows from Theorem 2 from [13], which states that if each agent's cost function depends only on their own states and actions, then the underlying game is

a constrained dynamic potential game. It is easy to see that agent costs according to (3) depend only on the individual agent's own states and control inputs. Therefore, we can use the results from Theorem 2 from [13] to obtain the potential function of the game \mathcal{G} to be

$$\sum_{i=1}^N \left(\frac{1}{2} \|x_\tau^i - \hat{x}_\tau^i\|_{Q_\tau^i}^2 + \frac{1}{2} \sum_{t=0}^{\tau-1} \|x_t^i - \hat{x}_t^i\|_{Q^i}^2 + \frac{1}{2} \sum_{t=0}^{\tau} \|u_t^i\|_{R^i}^2 \right). \quad (6)$$

Furthermore, using the joint notations, we can rewrite the sums in (6) as $\sum_{i=1}^N \left(\frac{1}{2} \|x_\tau^i - \hat{x}_\tau^i\|_{Q_\tau^i}^2 \right) = \frac{1}{2} \|x_\tau - \hat{x}_\tau\|_{Q_\tau}^2$, $\sum_{i=1}^N \left(\frac{1}{2} \|x_t^i - \hat{x}_t^i\|_{Q^i}^2 \right) = \frac{1}{2} \|x_t - \hat{x}_t\|_Q^2$, $\sum_{i=1}^N \left(\frac{1}{2} \|u_t^i\|_{R^i}^2 \right) = \frac{1}{2} \|u_t\|_R^2$. which in turn gives us (5).

Therefore, we have proven that \mathcal{G} is a constrained trajectory potential game with potential (5). Hence, using Theorem 2 from [13], any local solution of (5) will also be a local GNE of the game \mathcal{G} . \square

Therefore, using Theorem 1, finding local GNE trajectories is equivalent to finding local solutions to (5). The conventional approach to solving the optimization in (5) relies on techniques such as inter-point methods [23] or sequential quadratic programming [24]. Naively, the local solutions can be obtained by exhaustive initialization of random trajectories to an optimization solver, such as IPOPT [23], hoping to explore the solution space of local Nash equilibria. However, random exploration using gradient-based methods becomes computationally prohibitive for large N and inefficient as the same local equilibria can be arrived at from multiple random initializations. To address this, we utilize a Bayesian inference perspective in the following section to recover all local minima of (5) in an efficient manner.

V. IDENTIFYING LOCAL NASH EQUILIBRIA VIA BAYESIAN INFERENCE

In this section, we propose our approach to solve (5) from a Bayesian inference perspective. We reformulate the optimal control problem (5) into an equivalent Bayesian inference problem by utilizing the reference trajectory and constraint violations as virtual measurements that provide evidence for the optimal inference of the system trajectory in (5). At its core, the Bayesian inference problem is about approximating the probability density function (PDF) of the trajectories given measurement information derived from the objective and constraints in (5). Then, the high probability regions of the PDF to be approximated will correspond to the local GNEs of interest. This enables using the sample efficient implicit particle filter [30], which is designed to sample from the high probability regions of the PDF. The resulting identified equilibria then serve as a warm-start initialization for a downstream optimizer such as IPOPT, which finds the fine-tuned trajectory. We first formulate the *MultiNash-PF* problem and then outline the algorithm that realizes the framework.

A. MultiNash-PF framework via Bayesian Inference

Given problem (5), we view the objective function and constraints as a source of optimality information to facili-

tate the inference of the optimal trajectory. This motivates the introduction of a state-space model that sets us up to construct the Bayesian reformulation as a joint state and control inference via the objective function and constraint as measurements. We construct the virtual system as

$$\begin{aligned} x_{t+1} &= f(x_t, u_t), & y_{x,t} &= x_t + v_t, \\ u_{t+1} &= w_t, & y_{g,t} &= \psi(g(x_t, u_t)) + \eta_t, \end{aligned} \quad (7)$$

for $0 \leq t \leq \tau$, where x_t and u_t are the states of the virtual system, $y_{x,t}$, $y_{g,t}$ are measurements, and v_t , w_t , and η_t are bounded disturbances. The function $\psi(\cdot)$ represents a barrier function that can capture the degree of constraint violation by a trajectory. We chose the softplus barrier function for its continuity in the forthcoming filtering algorithm. The softplus function is expressed as:

$$\psi(g(x_t, u_t)) = \ln(1 + \exp(g(x_t, u_t))) / \alpha, \quad (8)$$

where α is a tuneable parameter that controls the strictness of enforcing constraints. Considering the virtual system (7), we relax the problem (5) using soft constraints as:

$$\begin{aligned} \min_{\{v_t, w_t, \eta_t\}_{t=0}^{\tau}} \quad & \frac{1}{2} \|v_{\tau}\|_{Q_{\tau}}^2 + \frac{1}{2} \sum_{t=0}^{\tau-1} \|v_t\|_Q^2 \\ \text{s.t.} \quad & + \frac{1}{2} \sum_{t=0}^{\tau} \|w_t\|_R^2 + \frac{1}{2} \sum_{t=0}^{\tau} \|\eta_t\|_{Q_{\eta}}^2, \\ & \begin{bmatrix} x_0 \\ u_0 \end{bmatrix} = \begin{bmatrix} \hat{x}_0 \\ w_{-1} \end{bmatrix}, \begin{bmatrix} x_{t+1} \\ u_{t+1} \end{bmatrix} = \begin{bmatrix} f(x_t, u_t) \\ 0_m \end{bmatrix} + \begin{bmatrix} 0_n \\ w_t \end{bmatrix}, \\ & \begin{bmatrix} y_{x,t} \\ y_{g,t} \end{bmatrix} = \begin{bmatrix} x_t \\ \phi(g(x_t, u_t)) \end{bmatrix} + \begin{bmatrix} v_t \\ \eta_t \end{bmatrix}, 0 \leq t \leq \tau, \end{aligned} \quad (9)$$

where Q_{η} is a positive definite weight matrix that assigns the importance of constraint satisfaction. Problem (9) differs from (5) in that it considers a soft inequality constraint using the barrier function (8). Further, (9) is also known as the moving horizon estimation problem [31] which aims to find the minima of the disturbances $\{v_t^*, w_t^*, \eta_t^*\}_{t=0}^{\tau}$. A direct attempt at solving (9) using traditional gradient-based methods poses a similar computational burden in identifying local Nash equilibria compared to problem (5). However, the above connection between (5) and the moving horizon estimation problem (9) highlights the potential to treat the problem from a Bayesian inference perspective. It can be seen that the constraints in (9) are the same as the considered virtual system in (7), suggesting that state inference can be performed via efficient estimation methods. To proceed, we rewrite (7) compactly as

$$\bar{x}_{t+1} = \bar{f}(\bar{x}_t) + \bar{w}_t, \quad \bar{y}_t = \bar{h}(\bar{x}_t) + \bar{v}_t, \quad (10)$$

$$\begin{aligned} \text{where} \quad & \bar{x}_t = \begin{bmatrix} x_t \\ u_t \end{bmatrix}, \quad \bar{y}_t = \begin{bmatrix} y_{x,t} \\ y_{g,t} \end{bmatrix}, \quad \bar{w}_t = \begin{bmatrix} 0_n \\ w_t \end{bmatrix}, \\ & \bar{v}_t = \begin{bmatrix} v_t \\ \eta_t \end{bmatrix}, \quad \bar{f}(\bar{x}_t) = \begin{bmatrix} f(x_t, u_t) \\ 0_m \end{bmatrix}, \quad \bar{h}(\bar{x}_t) = \begin{bmatrix} x_t \\ \psi(g(x_t, u_t)) \end{bmatrix}. \end{aligned}$$

Here, we relax \bar{w}_t and \bar{v}_t for $0 \leq t \leq \tau$ to be stochastic disturbances modeled as normally distributed random variables with PDF

$$\bar{v}_t \sim \mathcal{N}(0_{n+c}, \bar{Q}), \quad \bar{v}_{\tau} \sim \mathcal{N}(0_{n+c}, \bar{Q}_{\tau}), \quad \bar{w}_t \sim \mathcal{N}(0_{n+m}, \bar{R}), \quad (11)$$

with $\bar{Q} := \text{blkdiag}(Q^{-1}, Q_{\eta}^{-1})$, $\bar{Q}_{\tau} := \text{blkdiag}(Q_{\tau}^{-1}, Q_{\eta}^{-1})$, $\bar{R} := \text{blkdiag}(0_{n \times n}, R^{-1})$. The state estimation relevant to (10) is to estimate the state \bar{x}_t given the measurements \bar{y}_t . We must set the virtual measurement's value to correspond to the objective of the optimization in (5). We achieve this by noting that $y_{x,t}$ is a measurement value used to correct the state estimate of x_t towards the reference \hat{x}_t . While $y_{g,t}$ is to satisfy constraints through (8). Further, we observe that the barrier function in (8) outputs zero when the constraints are satisfied. Hence, the virtual measurement that will drive \bar{x}_t towards optimality takes the value

$$\bar{y}_t = \begin{bmatrix} \hat{x}_t \\ 0_c \end{bmatrix}, \quad 0 \leq t \leq \tau.$$

The Bayesian inference problem pertaining to (10) is to characterize the conditional PDF $p(\bar{x}_{0:\tau} | \bar{y}_{0:\tau})$. In the following, lemma (1) elucidates that characterizing the maximum a posteriori estimate of $p(\bar{x}_{0:\tau} | \bar{y}_{0:\tau})$ holds equivalence to solving (5).

Lemma 1. *Assuming independence between the noise vectors \bar{v}_t and \bar{w}_t in (11), the problem in (5) has the same optima as*

$$\bar{x}_{0:\tau}^* = \arg \max_{\bar{x}_{0:\tau}} \log p(\bar{x}_{0:\tau} | \bar{y}_{0:\tau}).$$

, We refer the interested reader to [12, Thm. 1] for the proof. The above lemma implies that the local GNEs in (5) translate to multiple local maxima of $p(\bar{x}_{0:\tau} | \bar{y}_{0:\tau})$. Hence, the Bayesian inference problem for (10) involves characterizing the multi-modal PDF $p(\bar{x}_{0:\tau} | \bar{y}_{0:\tau})$. Generally, state estimation of a multi-modal PDF does not admit closed-form solutions [32]. Hence, we resile to approximate solutions. A powerful approach is to use Monte Carlo methods that empirically approximate the distribution via a set of J particles as

$$p(\bar{x}_{0:\tau} | \bar{y}_{0:\tau}) \approx \sum_{j=1}^J w_j^i \delta(x_{0:\tau} - x_{0:\tau}^j), \quad (12)$$

where $\delta(\cdot)$ is the dirac delta function and w_j^i is the weight assigned to a sample trajectory $\bar{x}_{0:\tau}^i$ for $j = 1, \dots, J$. After identifying the local GNE through the above approximation, we extract the trajectories that appear as local GNE and use them to initialize an optimization solver. This completes the exposition of the *MultiNash-PF* framework.

We employ the implicit particle filter [30] due to its two-fold benefit for implementing the *MultiNash-PF* framework. First, as suggested in lemma 1, the local maxima (i.e high-probability regions) of $p(\bar{x}_{0:\tau} | \bar{y}_{0:\tau})$ correspond to the local GNEs. Hence, focusing our sampling efforts towards these high-probability regions can reduce the required samples for the approximation in (12). Second, we want to avoid the traditionally needed resampling step in particle filtering methods to ensure that the inferred trajectories are smooth. Fortunately, the implicit particle filter satisfies both of the aforementioned criteria. We leverage the Markovian property of the virtual system (10) to approximate (12). Using the Bayes' rule, we have

$$p(\bar{x}_{0:t} | \bar{y}_{0:t}) = p(\bar{y}_t | \bar{x}_t) p(\bar{x}_t | \bar{x}_{t-1}) p(\bar{x}_{0:t-1} | \bar{y}_{0:t-1}), \quad (13)$$

for $0 \leq t \leq \tau$. This indicates that given the particle \bar{x}_{t-1}^j from the prior distribution $p(\bar{x}_{0:t-1} | \bar{y}_{0:t-1})$, we can recursively obtain \bar{x}_t^j , reducing the complexity involved in directly sampling from a high-dimensional PDF. As shown in [30], we use implicit importance sampling and identify an implicit mapping to sample from high probability regions of (13). For this purpose, we make a local Gaussian assumption around \bar{x}_{t-1}^j such that

$$p(\bar{x}_t^j | \bar{y}_{0:t}) \sim \mathcal{N} \left(\hat{m}_t^j, \hat{\Sigma}_t^{x,j} \right), \quad (14)$$

where \hat{m}_t^j and $\hat{\Sigma}_t^{x,j}$ are the mean and error covariance of \bar{x}_t^j , respectively. These quantities are then found recursively by using a nonlinear Kalman filter. Then, the implicit map $X(\gamma_t^j)$ can be computed in closed form as

$$\bar{x}_t^j = \hat{m}_t^j + \sqrt{\hat{\Sigma}_t^{x,j}} \gamma_t^j, \quad (15)$$

where γ_t^j is a sample from $\mathcal{N}(0, I_n)$ and I_n denotes the identity matrix of size n .

Algorithm 1 MultiNash-PF: Multiple local GNEs based on particle filter

```

1: Formulate the constrained dynamic potential game (5)
2: Setup the virtual model (10)
   Perform unscented implicit particle filtering as follows:
3: Initialize the particles:  $\bar{x}_0^j$ ,  $\hat{\Sigma}_0^{x,j}$ , and  $w_0^j$  for  $j = 1, \dots, J$ 
4: for  $t = 0, 1, \dots, \tau - 1$  do
5:   for  $i = 1, 2, \dots, J$  do
   Run Kalman prediction step:
6:    $(m_{t+1}^j, \Sigma_{t+1}^{x,j}) \leftarrow \text{UT}(\bar{x}_t^j, \Sigma_t^{x,j}, \bar{R}, \bar{f})$ 
   Run Kalman update step:
7:   if  $t \leq \tau - 2$  then
8:      $(\hat{y}_{t+1}^j, \Sigma_{t+1}^{y,j}, \Sigma_{t+1}^{xy,j}) \leftarrow$ 
    $\text{UT}(m_{t+1}^j, \Sigma_{t+1}^{x,j}, \bar{Q}, \bar{h})$ 
9:   else
10:     $(\hat{y}_{t+1}^j, \Sigma_{t+1}^{y,j}, \Sigma_{t+1}^{xy,j}) \leftarrow$ 
    $\text{UT}(m_{t+1}^j, \Sigma_{t+1}^{x,j}, \bar{Q}_\tau, \bar{h})$ 
11:   end if
12:    $K_{t+1}^j \leftarrow \Sigma_{t+1}^{xy,j} (\Sigma_{t+1}^{y,j})^{-1}$ 
13:    $\hat{m}_{t+1}^{x,j} = m_{t+1}^j + K_{t+1}^j (\bar{y}_{t+1} - \hat{y}_{t+1}^j)$ 
14:    $\hat{\Sigma}_{t+1}^{x,j} \leftarrow \Sigma_{t+1}^{x,j} - K_{t+1}^j \Sigma_{t+1}^{y,j} (K_{t+1}^j)^\top$ 
   Draw a high-probability sample  $\gamma_{t+1}^j \sim \mathcal{N}(0, I_n)$  for the
   implicit mapping in (15):
15:    $\bar{x}_{t+1}^j \leftarrow \hat{m}_{t+1}^{x,j} + \sqrt{\hat{\Sigma}_{t+1}^{x,j}} \gamma_{t+1}^j$ 
   Weight and normalize samples:
16:    $w_{t+1}^j = \frac{w_t^j p(\bar{y}_{t+1} | \bar{x}_t^j)}{\sum_{j=1}^J w_t^j p(\bar{y}_{t+1} | \bar{x}_t^j)}, \quad p(\bar{y}_{t+1} | \bar{x}_t^j) \sim$ 
    $\mathcal{N}(\hat{y}_{t+1}^j, \Sigma_{t+1}^{y,j})$ 
17:   end for
18:   Perform resampling if necessary
19: end for
20: Extract trajectories from  $\{\bar{x}_{0:\tau}\}_{j=1}^J$  and warm start
   IPOPT solver to obtain the local GNEs  $\{x_{0:\tau}^{i*}, u_{0:\tau}^{i*}\}_{i=1}^N$ 
   of  $\mathcal{G}$ .

```

B. Implicit Particle Filter via Unscented Kalman filter

As in [30], we note that the local Gaussian approximation in (14) can be recursively computed through a nonlinear Kalman filter evolving according to (13) for all $j = 1, \dots, J$.

Our nonlinear Kalman filter of choice is the unscented Kalman filter due to its high filtering accuracy for low-dimensional state space models [33]. The unscented Kalman filter is based on the unscented transform, which utilizes deterministic samples, known as sigma points, to trace the evolution of the mean and covariance of a Gaussian random variable through a nonlinear function. The unscented Kalman filter [33] utilizes the unscented transform in the Kalman prediction and measurement update steps to keep track of the Gaussian statistics through the state transition and measurement function in (10). From now on, we use **UT** to denote Unscented Transform algorithm.

Using the unscented Kalman filter, we can recursively compute the local Gaussian approximation (14) at time t . Then, we implicitly map the particle to the high-probability regions by sampling $\gamma_t^i \sim \mathcal{N}(0, I_n)$ for (15) to obtain the particle \bar{x}_t^i . If necessary, we perform resampling for the particle trajectory $\bar{x}_{0:t}^i$. This process is repeated until $t = \tau$ for each particle to obtain the set of trajectories $\{\bar{x}_{0:\tau}\}_{j=1}^J$, which will include the coarse estimates of local GNEs. This completes the unscented implicit particle filter, which has identified the coarse estimates of multiple local Nash equilibria in (5). As the last step, the estimates of local equilibria are extracted and used as warm start initialization to the IPOPT optimizer to find the optimal local GNEs. To extract the equilibria, we carefully observe the trajectories and select the trajectories that are repeatedly taken by multiple particles. The pragmatic extraction of equilibria from the particle trajectories is nontrivial and is left for future study. The implementation details of the proposed *MultiNash-PF* through the unscented implicit particle filter are provided in Algorithm 1.

VI. NUMERICAL SIMULATIONS

To showcase the capabilities of our method, we take motivation from real-life highway scenarios. We first consider an interaction between two agents moving toward each other as shown in Fig 1. We consider the following discrete-time unicycle dynamics to model each agent $i \in \{1, 2\}$:

$$p_{t+1}^i = p_t^i + \Delta t \cdot v_t^i \cos \theta_t^i, \quad q_{t+1}^i = q_t^i + \Delta t \cdot v_t^i \sin \theta_t^i$$

$$\theta_{t+1}^i = \theta_t^i + \Delta t \cdot \omega_i, \quad v_{t+1}^i = v_t^i + \Delta v_t^i, \quad \omega_{t+1}^i = \omega_t^i + \Delta \omega_t^i,$$

where Δt is the time-step size, p_t^i and q_t^i are x and y coordinates of the positions, θ_t^i is the heading angle from positive x-axis, v_t^i is the linear velocity, and ω_t^i is the angular velocity of the agent i at time t . Further, Δv_t^i is the change in linear velocity, and $\Delta \omega_t^i$ is the change in angular velocity of the agent i at time t , respectively. For each agent i , we denote the state vector x_t^i and the action vector u_t^i as follows

$$x_t^i = [p_t^i \quad q_t^i \quad \theta_t^i \quad v_t^i \quad \omega_t^i]^\top, \quad u_t^i = [\Delta v_t^i \quad \Delta \omega_t^i]^\top.$$

We formulate this scenario as a two-player game according to cost functions as described in (3). The reference trajectory for both agents is given as a straight line on the highway, starting from their initial position to their respective goal location. With $\bar{Q} = \text{diag}(50, 10, 5, 5, 2)$, the reference tracking and control effort cost matrices are set as

$$Q^i = 0.6\bar{Q}, \quad Q_\tau^i = 100\bar{Q}, \quad R^i = \text{diag}(8, 4). \quad (16)$$

for $i \in \{1, 2\}$. In addition, the agents are subject to the constraint of avoiding collision with each other, which we define as

$$g_c(x_t, u_t) := -d(x_t^1, x_t^2) + r_{\text{col}} \leq 0, \quad (17)$$

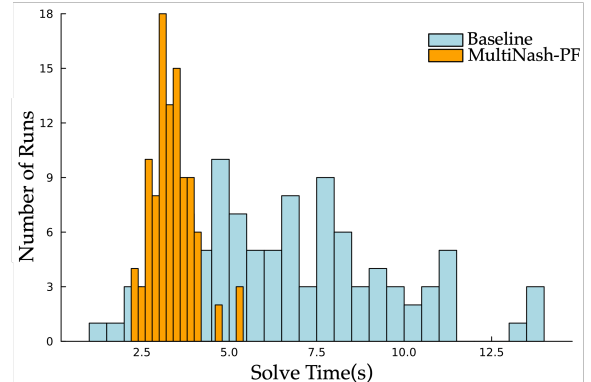
where $d(x_t^1, x_t^2) := \sqrt{(p_t^1 - p_t^2)^2 + (q_t^1 - q_t^2)^2}$ is the Euclidean distance between the two agents and $r_{\text{col}} := 3m$ is the collision avoidance radius between the two agents.

With this setup, we employ MultiNash-PF from Algorithm 1 to efficiently capture the multi-modality in the solution space and then extract the solutions to provide a warm start trajectory to a solver like IPOPT [23] to recover different local GNEs. We use the Julia programming language and utilize the JuMP [34] library to solve the game using IPOPT solver. The results of our method are provided in Fig 1. As we can see, the presence of two agents and collision avoidance constraints induces two different possible Nash equilibria. Either both the agents will yield to their right, or they will yield to their left to avoid collision. As shown in Fig 1, our method can recover both equilibria.

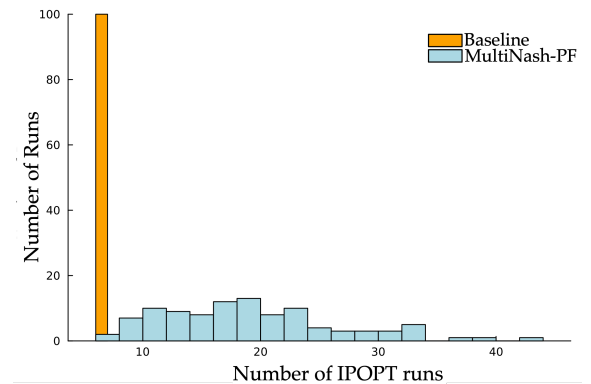
Furthermore, we consider a more complicated scenario in which two agents aim to exchange their positions while avoiding an obstacle of radius $r_{\text{obs}} = 4m$ located at the midpoint of the two agents. It should be noted that the radius of the obstacle is larger than the collision avoidance radius of the two agents.

We consider the same unicycle dynamics as before, and the reference trajectory cost is also the same as in (16). Furthermore, the collision avoidance radius between the two agents is also the same as before. In addition to (17), the constraints for this game will include both agents avoiding the obstacle $g_o^i(x_t, u_t) := [-d(x_t^i, x_{\text{obs}}) + r_{\text{obs}}]$ for $i = 1, 2$ where x_{obs} is the location of the obstacle. We also assume that we have constraints on the control bounds $g_b(x_t, u_t) = [-v_t^1, -v_t^2, |u_t^1| - u_b^1, |u_t^2| - u_b^2]$, where u_b^1 and u_b^2 are controlled action bounds for agents 1 and 2, respectively. We write the combined constraints as $g(x_t, u_t) := [g_c \ g_o^1 \ g_o^2 \ g_b]^\top \leq 0$. We choose the values of control action bounds to be $u_b^1 = u_b^2 = [0.15, 0.75]^\top$. This setup induces multitudes of local equilibria. Two trivial local equilibria are when the two agents pass each other through opposite sides of the obstacle. However, there exist four other nontrivial equilibria when both agents can go on the same side of the obstacle, and one of the agents can yield to the other one. It is challenging to recover all six equilibria without utilizing the capabilities of the implicit particle filter. Upon performing simulation experiments with our method, we observe that MultiNash-PF is able to recover all six Nash equilibria as shown in Fig. 2.

1) *Comparison with Baseline*: In order to compare the effectiveness of our method, we consider a baseline method. In the baseline method, we directly initialize the IPOPT solver with random perturbations of reference trajectories and compute the resulting optimal solutions. For our method, we fixed $J = 50$ particles and obtained the solution trajectories using implicit particle filtering from Algorithm 1 described in Section V. After that, we extract all the different



(a) Histogram of the solve time comparison of MultiNash-PF and the baseline.



(b) Histogram of the number of the IPOPT runs required to obtain all six equilibria.

Fig. 3: Histograms of the comparison of MultiNash-PF with the baseline for the experiment shown in Fig. 2.

(a) The average solve time for MultiNash-PF is 3.36 ± 0.59 s while the baseline's average solve time is 6.71 ± 2.83 s. MultiNash-PF reduces the solve time by about 50% compared to the baseline while giving a much lower variance on the solve time. (b) For the baseline, the average number of IPOPT runs required to obtain all six different equilibria is 18.64 ± 7.57 , while for MultiNash-PF, this is always 6. MultiNash-PF requires 3 times fewer IPOPT runs.

equilibria and provide them as a warm starting point for IPOPT to obtain the final solutions. The compute time of our method is a combination of time used in implicit particle filtering and time used by IPOPT to obtain all the different equilibria given warm starting from filtering.

We run the IPOPT solver until we recover all 6 different equilibria. We repeat this experiment for 100 different Monte Carlo runs. We observe that it requires, on average, 18.64 ± 7.57 number of IPOPT runs to obtain all six different equilibria using the baseline approach of random warm-starting. However, with our method, the number of IPOPT runs required is always six because we always obtain all six modes of equilibria from implicit particle filtering. A histogram of the number of IPOPT runs required for obtaining all six equilibria is plotted in Fig. 3b.

Furthermore, the solve time to recover all 6 different Nash equilibria for the baseline is 6.71 ± 2.83 s, while for MultiNash-PF, the solve time is 3.36 ± 0.59 s. Our

method results in a solve-time reduction of 50% compared to the baseline while giving a much lower variance on the solve time. A histogram of the solve times of the baseline compared to our method is plotted in Fig. 3a. As explained earlier, our method's solve time is a combination of the time used in implicit particle filtering and the time used by IPOPT. We observe that the time required for implicit particle filtering over 100 Monte Carlo runs is 0.37 ± 0.072 s while the time used by IPOPT to obtain the final solutions is 2.99 ± 0.57 s. Therefore, in our MultiNash-PF, the time used by implicit particle filtering is 11% of the total solve time, which shows that filtering is very efficient in exploring the solution space of local Nash equilibria and contributes really less to the overall computation time of MultiNash-PF.

VII. CONCLUSION

In this work, we introduced MultiNash-PF, a novel algorithm designed to efficiently compute multiple local generalized Nash equilibria (GNEs) in constrained trajectory games. By integrating potential game theory with implicit particle filtering, MultiNash-PF provides coarse estimates of local minimizers, which are then refined using off-the-shelf optimization solvers. Our experimental results in two-player trajectory games involving nonlinear dynamics and collision avoidance constraints demonstrate that MultiNash-PF not only identifies all local Nash equilibria but also significantly reduces computation time compared to traditional random initialization methods. This enhanced efficiency and accuracy underline the potential of MultiNash-PF to improve identifying various interaction modes in complex, real-world environments, paving the way for more robust and socially acceptable autonomous systems.

REFERENCES

- [1] T. Başar and G. J. Olsder, *Dynamic noncooperative game theory*. SIAM, 1998.
- [2] G. Galati, S. Primatesta, S. Grammatico, S. Macrì, and A. Rizzo, “Game theoretical trajectory planning enhances social acceptability of robots by humans,” *Scientific Reports*, vol. 12, no. 1, p. 21976, 2022.
- [3] D. Sadigh, S. Sastry, S. A. Seshia, and A. D. Dragan, “Planning for autonomous cars that leverage effects on human actions.,” in *Robotics: Science and systems*, vol. 2, pp. 1–9, Ann Arbor, MI, USA, 2016.
- [4] D. Fridovich-Keil, V. Rubies-Royo, and C. J. Tomlin, “An iterative quadratic method for general-sum differential games with feedback linearizable dynamics,” in *2020 IEEE International Conference on Robotics and Automation (ICRA)*, pp. 2216–2222, IEEE, 2020.
- [5] A. Dreves and M. Gerdtz, “A generalized Nash equilibrium approach for optimal control problems of autonomous cars,” *Optimal Control Applications and Methods*, vol. 39, no. 1, pp. 326–342, 2018.
- [6] M. Wang, N. Mehr, A. Gaidon, and M. Schwager, “Game-theoretic planning for risk-aware interactive agents,” in *2020 IEEE/RSJ International Conference on Intelligent Robots and Systems (IROS)*, pp. 6998–7005, IEEE, 2020.
- [7] L. Peters, D. Fridovich-Keil, C. J. Tomlin, and Z. N. Sunberg, “Inference-based strategy alignment for general-sum differential games,” *arXiv preprint arXiv:2002.04354[cs.RO]*, 2020.
- [8] J. Im, Y. Yu, D. Fridovich-Keil, and U. Topcu, “Coordination in noncooperative multiplayer matrix games via reduced rank correlated equilibria,” *arXiv preprint arXiv:2403.10384[cs.GT]*, 2024.
- [9] C. Daskalakis, P. W. Goldberg, and C. H. Papadimitriou, “The complexity of computing a Nash equilibrium,” *Communications of the ACM*, vol. 52, no. 2, pp. 89–97, 2009.
- [10] F. Facchinei and C. Kanzow, “Generalized Nash equilibrium problems,” *Annals of Operations Research*, vol. 175, no. 1, pp. 177–211, 2010.
- [11] S. Zazo, S. V. Macua, M. Sánchez-Fernández, and J. Zazo, “Dynamic potential games with constraints: Fundamentals and applications in communications,” *IEEE Transactions on Signal Processing*, vol. 64, no. 14, pp. 3806–3821, 2016.
- [12] I. Askari, X. Tu, S. Zeng, and H. Fang, “Model predictive inferential control of neural state-space models for autonomous vehicle motion planning,” *arXiv preprint arXiv:2310.08045*, 2023.
- [13] M. Bhatt, Y. Jia, and N. Mehr, “Efficient constrained multi-agent trajectory optimization using dynamic potential games,” in *2023 IEEE/RSJ International Conference on Intelligent Robots and Systems (IROS)*, pp. 7303–7310, IEEE, 2023.
- [14] S. M. LaValle, “Robot motion planning: A game-theoretic foundation,” *Algorithmica*, vol. 26, pp. 430–465, 2000.
- [15] A. Liniger and J. Lygeros, “A noncooperative game approach to autonomous racing,” *IEEE Transactions on Control Systems Technology*, vol. 28, no. 3, pp. 884–897, 2019.
- [16] R. Spica, E. Cristofalo, Z. Wang, E. Montijano, and M. Schwager, “A real-time game theoretic planner for autonomous two-player drone racing,” *IEEE Transactions on Robotics*, vol. 36, no. 5, pp. 1389–1403, 2020.
- [17] M. Wang, Z. Wang, J. Talbot, J. C. Gerdes, and M. Schwager, “Game theoretic planning for self-driving cars in competitive scenarios.,” in *Robotics: Science and Systems*, 2019.
- [18] D. Fridovich-Keil, E. Ratner, L. Peters, A. D. Dragan, and C. J. Tomlin, “Efficient iterative linear-quadratic approximations for nonlinear multi-player general-sum differential games,” in *2020 IEEE International Conference on Robotics and Automation (ICRA)*, pp. 1475–1481, IEEE, 2020.
- [19] S. Le Cleac'h, M. Schwager, and Z. Manchester, “Algames: a fast augmented lagrangian solver for constrained dynamic games,” *Autonomous Robots*, vol. 46, no. 1, pp. 201–215, 2022.
- [20] F. Laine, D. Fridovich-Keil, C.-Y. Chiu, and C. Tomlin, “The computation of approximate generalized feedback Nash equilibria,” *SIAM Journal on Optimization*, vol. 33, no. 1, pp. 294–318, 2023.
- [21] T. Kavuncu, A. Yaraneri, and N. Mehr, “Potential iLQR: A potential-minimizing controller for planning multi-agent interactive trajectories,” *arXiv preprint arXiv:2107.04926*, 2021.
- [22] Y. Jia, M. Bhatt, and N. Mehr, “Rapid: Autonomous multi-agent racing using constrained potential dynamic games,” in *2023 European Control Conference (ECC)*, pp. 1–8, IEEE, 2023.
- [23] A. Wächter and L. T. Biegler, “On the implementation of an interior-point filter line-search algorithm for large-scale nonlinear programming,” *Mathematical Programming*, vol. 106, no. 1, pp. 25–57, 2006.
- [24] P. T. Boggs and J. W. Tolle, “Sequential quadratic programming,” *Acta numerica*, vol. 4, pp. 1–51, 1995.
- [25] D. Stahl and J. Hauth, “Pf-mpc: Particle filter-model predictive control,” *Systems & Control Letters*, vol. 60, no. 8, pp. 632–643, 2011.
- [26] I. Askari, S. Zeng, and H. Fang, “Nonlinear model predictive control based on constraint-aware particle filtering/smoothing,” in *2021 American Control Conference (ACC)*, pp. 3532–3537, IEEE, 2021.
- [27] I. Askari, B. Badnava, T. Woodruff, S. Zeng, and H. Fang, “Sampling-based nonlinear MPC of neural network dynamics with application to autonomous vehicle motion planning,” in *2022 American Control Conference (ACC)*, pp. 2084–2090, IEEE, 2022.
- [28] A. Doucet, N. De Freitas, N. J. Gordon, *et al.*, *Sequential Monte Carlo methods in practice*, vol. 1. Springer, 2001.
- [29] S. Särkkä and L. Svensson, *Bayesian filtering and smoothing*, vol. 17. Cambridge university press, 2023.
- [30] I. Askari, M. A. Haile, X. Tu, and H. Fang, “Implicit particle filtering via a bank of nonlinear Kalman filters,” *Automatica*, vol. 145, p. 110469, 2022.
- [31] C. Rao, J. Rawlings, and D. Mayne, “Constrained state estimation for nonlinear discrete-time systems: stability and moving horizon approximations,” *IEEE Transactions on Automatic Control*, vol. 48, no. 2, pp. 246–258, 2003.
- [32] S. Särkkä, *Bayesian Filtering and Smoothing*. Institute of Mathematical Statistics Textbooks, 2013.
- [33] H. Fang, N. Tian, Y. Wang, M. Zhou, and M. A. Haile, “Nonlinear Bayesian estimation: from Kalman filtering to a broader horizon,” *IEEE/CAA Journal of Automatica Sinica*, vol. 5, no. 2, pp. 401–417, 2018.
- [34] I. Dunning, J. Huchette, and M. Lubin, “Jump: A modeling language for mathematical optimization,” *SIAM review*, vol. 59, no. 2, pp. 295–320, 2017.